Electronic Supplementary Information for

Bi$_2$Fe$_4$O$_9$@ZnIn$_2$S$_4$ S-scheme Laminated Heterojunction Photocatalyst Towards Optimized Photocatalytic Performance

Chunxu Wu[a], Zipeng Xing[a,*], Yichao Wang[a], Hui Peng[a], Weifeng Kong[a], Shilin Yang[a,*], Zhenzi Li[b], Wei Zhou[b,*]

[a] Department of Environmental Science, School of Chemistry and Materials Science, Key Laboratory of Functional Inorganic Material Chemistry, Ministry of Education of the People's Republic of China, Heilongjiang University, Harbin 150080, P. R. China, Tel: +86-451-8660-8616, Fax: +86-451-8660-8240,

Email: xingzipeng@hlju.edu.cn; yslchem@163.com

[b] Shandong Provincial Key Laboratory of Molecular Engineering, School of Chemistry and Chemical Engineering, Qilu University of Technology (Shandong Academy of Sciences), Jinan 250353, P. R. China

Email: zwchem@hotmail.com

Experimental section

1. Materials

Bismuth nitrate pentahydrate ($Bi(NO_3)_3 \cdot 5H_2O$), ferric chloride hexahydrate ($FeCl_3 \cdot 6H_2O$), sodium hydroxide (NaOH) and indium chloride tetrahydrate ($InCl_3 \cdot 4H_2O$) were purchased from Shanghai Aladdin Biochemical Technology Co., Ltd. Zinc chloride ($ZnCl_2$) and Thioacetamide (TAA) were purchased from Shanghai Macklin Biochemical Co., Ltd. Absolute ethanol (EtOH), ethylene glycol (($CH_2OH)_2$) and ammonia ($NH_3 \cdot H_2O$) were purchased from Tianjin Kermel Chemical Reagent Co., Ltd. All of the reagents which were used in the experiments were analytical grade and employed without further purification, and the deionized water was used throughout the study.

2. Characterizations

The as-synthesized samples were confirmed by powder X-ray diffraction (XRD) on a Bruker D8 advance under Cu Kα (λ = 1.5406 Å) radiation. The Fourier-transform infrared (FT-IR) spectra were collected with a Thermo Scientific Nicolet iS50 FT-IR spectrometer, KBr as the diluents. The microcrystalline structure, surface characteristics and element distribution of these samples were examined by scanning electron microscopy (SEM, Hitachi S-4800) with energy-dispersive X-ray spectrometer (EDX) operated at an accelerating voltage of 20 kV. Transmission electron microscopy (TEM) and high-resolution transmission (HRTEM) images were obtained by (FEI Tecnai F20) electron microscope at an accelerating voltage of 200 kV. The •OH were detected by the fluorescence probe technique with coumarin on a

RF-5301PC fluorescence spectrophotometer. X-ray photoelectron spectroscopy (XPS) was measured on a PHI-5700 ESCA instrument with Al-Kα X-ray source. In-situ irradiated XPS measurements of samples with external light source irradiation were performed on the basis of XPS measurements. The UV-vis diffuse reflection spectra (DRS) were recorded on a UV-vis spectrophotometer (UV-2550, Shimadzu) with an integrating sphere attachment, and $BaSO_4$ was used as the reference material. The work function was tested by Scanning Kelvin probe (SKP) (SKP5050 system, Scotland). Electron paramagnetic resonance (EPR) was performed on EPR spectrometer (MEX-nano, Bruker, German). The steady-state photoluminescence (PL) spectra were recorded on a fluorescence spectrophotometer (Fluorolog-Tau-3, America), excited at 372 nm. Specific surface area was estimated by Brunauer-Emmett-Teller (BET) method and pore-size distribution was measured from the adsorption branch of the isotherm using the Barrett-Joyner-Halenda (BJH) method.

3. Synthesis

3.1. Synthesis of $Bi_2Fe_4O_9$ nanosheets

$Bi_2Fe_4O_9$ nanosheets were synthesized through hydrothermal-annealing method. Typically, 2.425 g of $Bi(NO_3)_3·5H_2O$ was dissolved in 50 mL ethylene glycol. After stirring for 0.5 h, 1.352 g of $FeCl_3·6H_2O$ was added into the owned solution and stirred continuously. Subsequently, 200 mL deionized (DI) water and concentrated ammonia were added into the solution obtained in the previous step. The pH value of the solution was adjusted to be 10~11 by adding $NH_3·H_2O$ under vigorous stirring. The precipitate was centrifuged and collected and washed several times with DI water

until the pH reached approximately 7.0. The precipitate was again collected by centrifugation and then added to 40 mL of NaOH solution. Next the solution was transferred into a Teflon-lined stainless-steel autoclave and maintained at 150 °C for 6 h. The suspension was washed several times with DI water and ethanol and dried at 60 °C for 12 h. The $Bi_2Fe_4O_9$ nanosheets was obtained by calcination at 800 °C for 2 h in air atmosphere, which was named as BFO-6. In addition, in order to explore the optimal growth conditions of $Bi_2Fe_4O_9$, the hydrothermal time was adjusted to 2 h and 10 h, respectively, and other conditions were kept constant. Accordingly, the obtained samples were named as BFO-2 and BFO-10, respectively.

3.2. Synthesis of $Bi_2Fe_4O_9@ZnIn_2S_4$

$Bi_2Fe_4O_9@ZnIn_2S_4$ was prepared by hydrothermal method. Typically, 0.1 g prepared $Bi_2Fe_4O_9$ nanosheets (BFO-6) were dispersed in 100 mL bakers containing 50 mL DI water, then $ZnCl_2$ (0.136 g), TAA (0.15 g) and $InCl_3·4H_2O$ (0.293 g) were added into the bakers. After stirring for 0.5 h, the solution was transferred into a Teflon-lined stainless-steel autoclave and maintained at 160 °C for 12 h. The suspension was washed several times with DI water and ethanol. The final products were obtained by drying at 60 °C for 12 h, which was named as BFO@ZIS. The $ZnIn_2S_4$ nanosheets was synthesized under the same reaction conditions without the addition of $Bi_2Fe_4O_9$ nanosheets as the substrate, which was named as ZIS.

4. Photocatalytic degradation tests

Tetracycline was selected to test the photocatalytic degradation performance at room temperature. In a typical experiment, the photocatalysts (30 mg) was added to

tetracycline solution (30 mL, 10 mg L^{-1}). Then, the suspension was placed in the dark to ensure adsorption-desorption equilibrium. The suspension was irradiated with a 300 W Xenon lamp equipped with UVCUT filter ($\lambda \geq 420$ nm). The residual tetracycline concentrations were analyzed by T6 UV-vis spectrophotometer.

5. Photocatalytic hydrogen evolution

Photocatalytic H_2 evolution experiment was carried out in a photocatalytic hydrogen production system (AuLight, Beijing, CEL-SPH2N). In the photocatalytic hydrogen evolution reaction, 100 mg of catalyst powder was suspended in an aqueous solution (25 mL) containing Na_2S (0.35 M) and Na_2SO_3 (0.25 M) as sacrificial agent. Before visible light exposure, the reactor and the entire gas circulation system were completely degassed by vacuum pump to remove air for 30 min. The 300 W Xenon is then fitted with optical filter ($\lambda \geq 420$ nm) as a visible light source. The evolution of photocatalytic H_2 was analyzed by gas chromatograph (SP7800, TCD, molecular sieve 5a, N_2 carrier, Beijing Keruida Limited.).

6. Photoelectrochemical measurements

The electrochemical impedance spectroscopy and photocurrents curves were examined by the CHI760E electrochemical workstation, which employed the three-electrode configuration. Na_2SO_4 (0.1 M) aqueous solution was used as the electrolyte solution. Pt foil was the counter electrode and Ag/AgCl electrode was used as the reference electrode. In order to prepare working electrode, photocatalyst sample (50 mg) was dispersed in ethanol (3 mL). Then the suspension was sprayed onto the FTO glass and further heated and dried. The photocurrent curves were obtained by

equipping a 300 W Xenon lamp with UVIRCUT filter (420-780 nm). The frequencies of Mott-Schottky plot measurements were 500, 1000, and 1500 Hz, respectively. Electro-chemical impedance spectroscopy was measured with amplitude of 5 mV and frequencies varying from 0.01 to 10000 Hz.
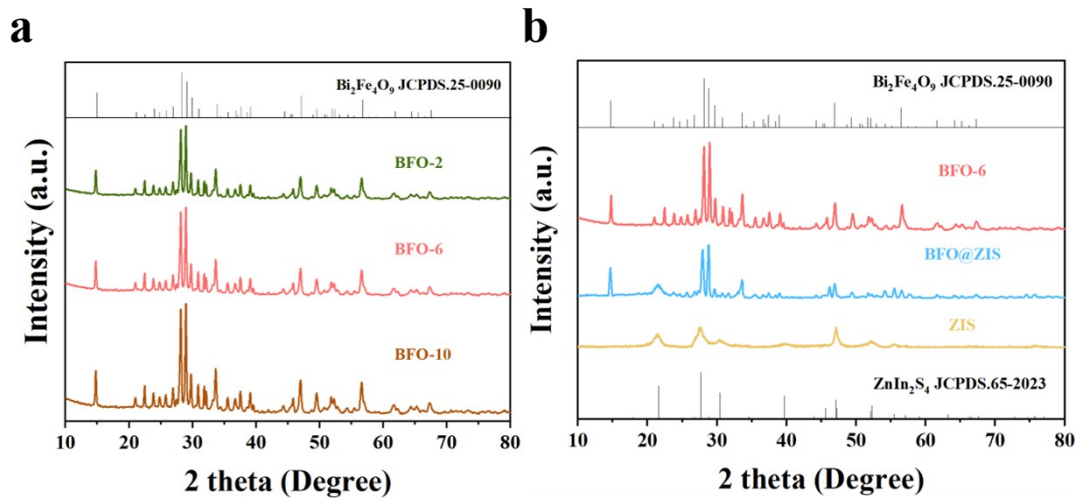
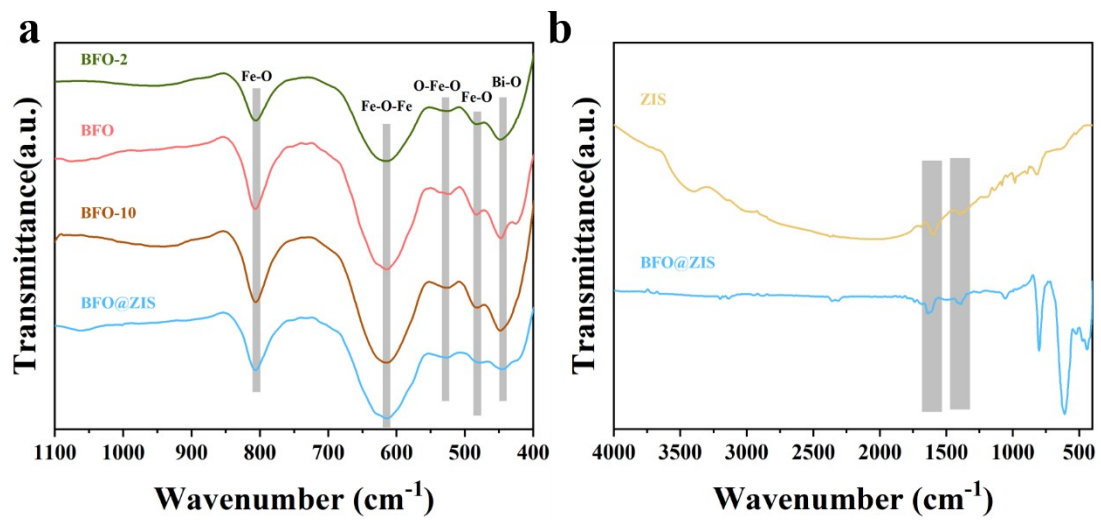**Fig. S1.** Typical XRD patterns of BFO-2, BFO-6 and BFO-10 (a), BFO-6, ZIS and BFO@ZIS (b).

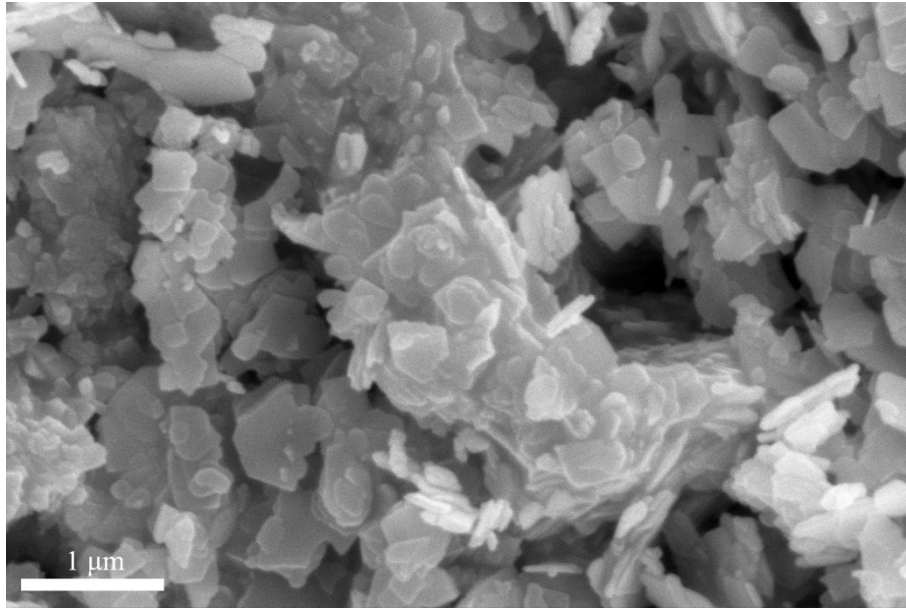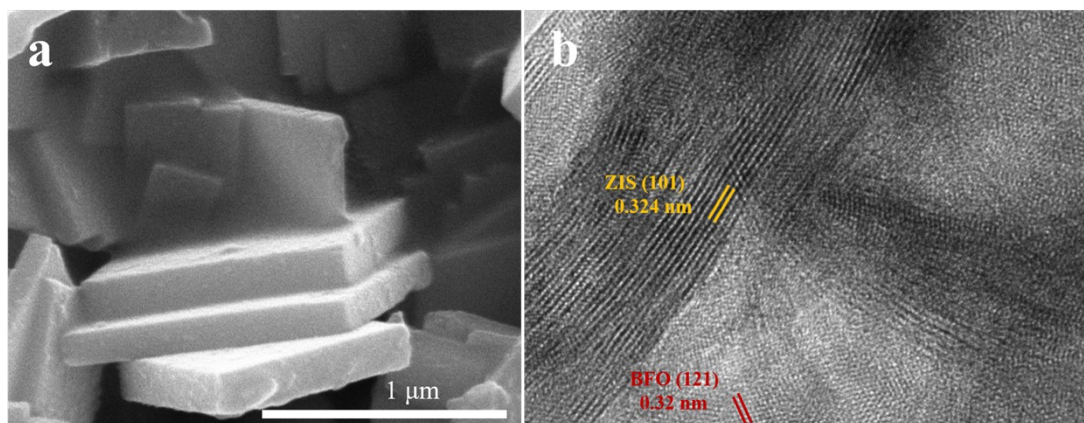**Fig. S2.** FT-IR spectra of BFO-2, BFO-6, BFO-10 and BFO@ZIS (a), ZIS and BFO@ZIS (b).

Fig. S3. The SEM image of BFO-2.

Fig. S4. The SEM image of BFO-10 (a) and HRTEM image of BFO@ZIS (b).
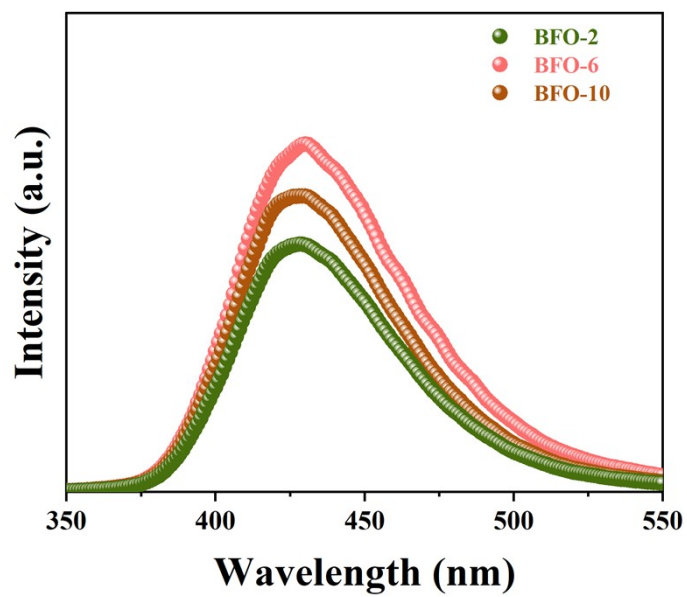
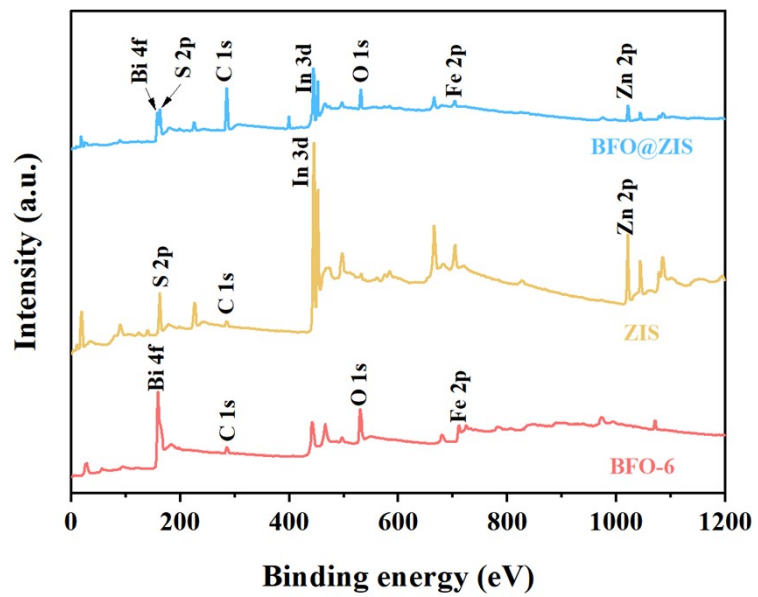**Fig. S5.** The hydroxyl radical amount-related fluorescence spectra of BFO-2, BFO-6 and BFO-10.

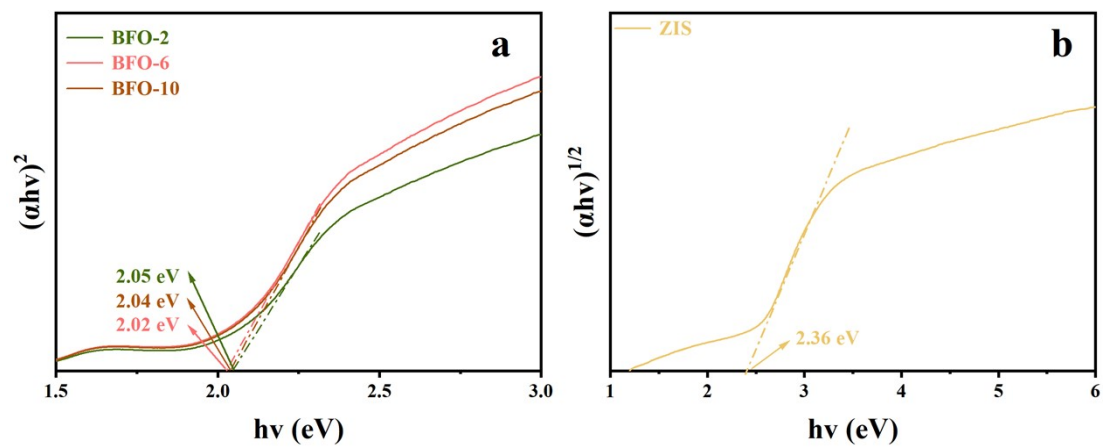**Fig. S6.** XPS full survey spectra of BFO-6, ZIS and BFO@ZIS, respectively.

Fig. S7. Typical Tauc plots for indirect band gaps of BFO-2, BFO-6 and BFO-10 (a) and ZIS (b).
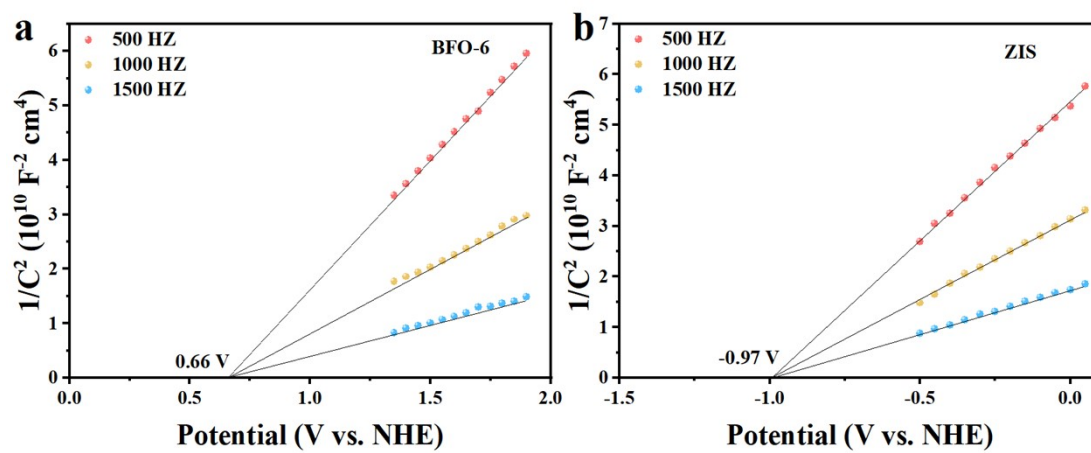
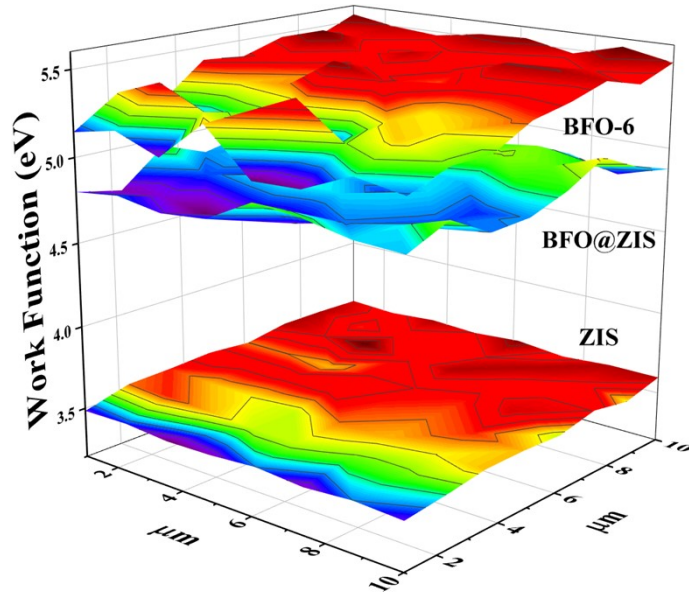**Fig. S8.** Mott-Schottky curves of BFO-6 (a) and ZIS (b), respectively.

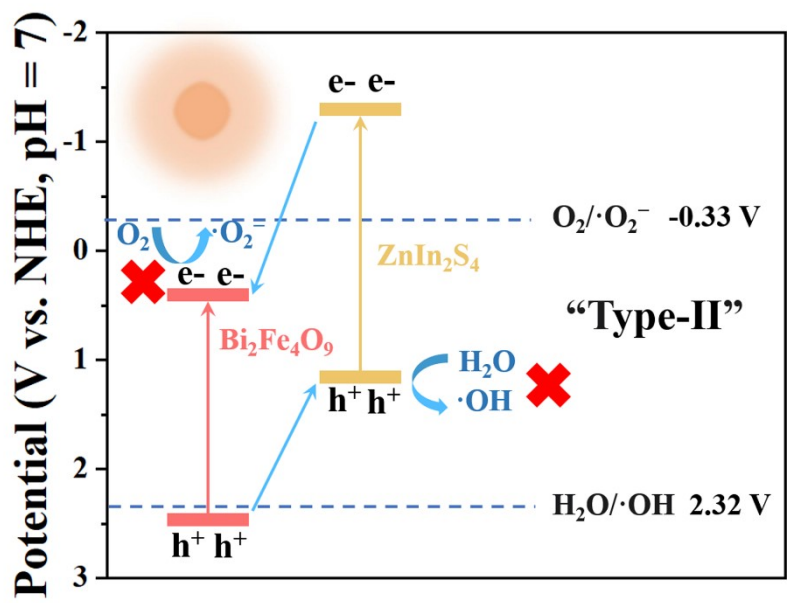**Fig. S9.** SKP maps of BFO-6, ZIS, and BFO@ZIS.

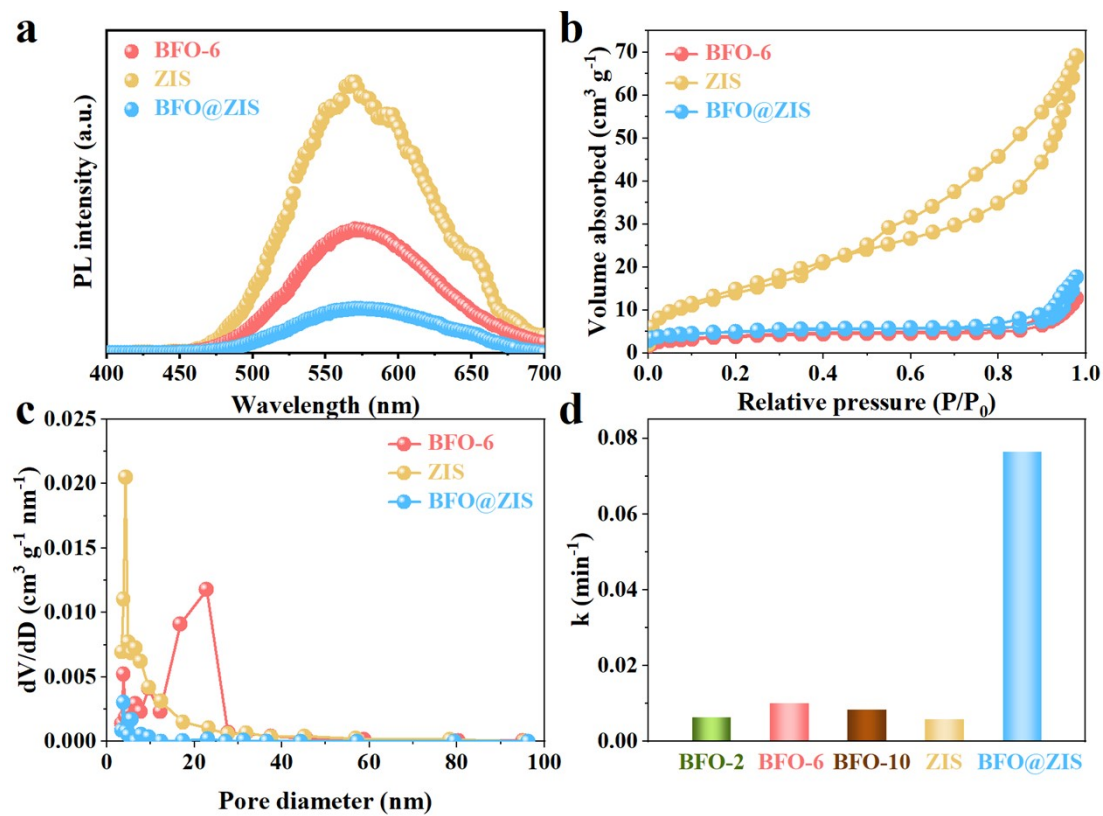**Fig. S10.** Schematic diagrams of type-II heterojunction.

Fig. S11. Steady-state PL spectra of BFO-6, ZIS and BFO@ZIS (a). Nitrogen adsorption/desorption isotherms (b), and corresponding BJH pore size distributions (c) of BFO-6, ZIS and BFO@ZIS and apparent reaction rate constants of all samples (d), respectively.
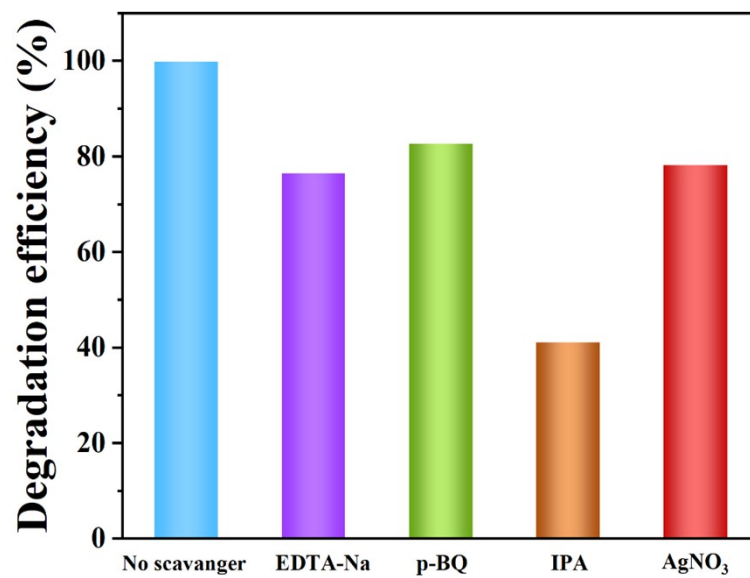
Fig. S12. The species trapping experiments for photocatalytic degradation of tetracycline over BFO@ZIS photocatalyst under visible light irradiation.

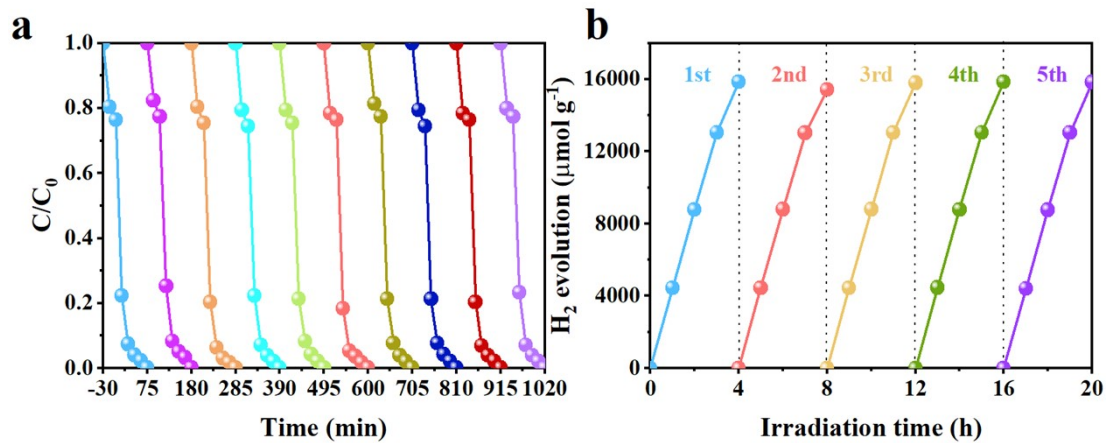**Fig. S13.** The recycling runs of BFO@ZIS for the degradation of tetracycline (a). Photocatalytic
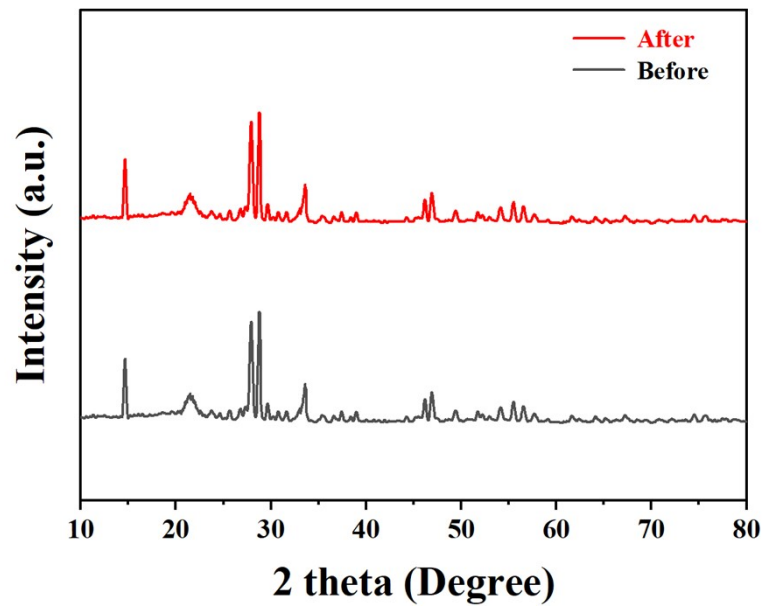
H_2 evolution cycle tests of BFO@ZIS (b).

Fig. S14. The XRD patterns of BFO@ZIS before and after the photocatalytic hydrogen production

experiments.

Table S1. Comparison of photocatalytic tetracycline degradation performance for BFO@ZIS and other photocatalysts.

Photocatalyst	Weight	Light source	Reaction time	Pollutant	Degradation efficiency	Ref.
oxygen-deficient Bi_2WO_6	30 mg	300 W Xe lamp $\lambda \geq 420$ nm	210 minutes	Tetracycline (100 mL, 20 mg/L)	79.68%	[1]
Sn-Bi-MOF/Ti_3C_2	40 mg	500 W Xe lamp	135 minutes	Tetracycline (30 mL, 20 mg/L)	96.2%	[2]
MIL-125(Mo)-In_2Se_3	10 mg	Xe lamp 780 nm $\geq \lambda \geq$ 350 nm	240 minutes	Tetracycline (40 mL, 50 mg/L)	94.14%	[3]
MnO_2/$BiVO_4$	20 mg	50 W halogen lamp $\lambda \geq 420$ nm	150 minutes	Tetracycline (100 mL, 5 g)	59%	[4]
$Bi_{28}O_{32}$ $(SO_4)_{10}$/NiAl LDH	30 mg	1 kW Xe lamp $\lambda \geq 400$ nm	150 minutes	Tetracycline (50 mL, 10 mg/L)	Around 95%	[5]
In_2S_3/Ta_2O_{5-x}	50 mg	300 W Xe lamp $\lambda \geq 400$ nm	2 hours/2 hours	Tetracycline (35 mg/L)	Around 55%	[6]
$BiPO_4$/Ag_3PO_4@rGO	30 mg	250 W Xe lamp $\lambda \geq 420$	105 minutes	Tetracycline (50 mL, 10 mg/L)	94.6%	[7]

		nm				
Bi$_2$Fe$_4$O$_9$@ZnIn$_2$S$_4$	30 mg	300 W Xe lamp λ ≥ 420 nm	105 minutes	Tetracycline (30 mL, 10 mg/L)	99.9%	This work

Table S2. Comparison of photocatalytic H_2 evolution performance for BFO@ZIS and other photocatalysts.

Photocatalysts	Light source	H_2 evolution rate ($\mu mol\ h^{-1}\ g^{-1}$)	References
N doped TiO_2	300 W Xe lamp $\lambda \geq 400$ nm	3183	[8]
$TiO_2/ZnIn_2S_4$	300 W Xe lamp	214.9	[9]
g-$C_3N_4/Co_3O_4/MoS_2$	$\lambda \geq 400$ nm	105	[10]
Se-modified m-CNNSs	300 W Xe lamp	130	[11]
$SiO_2@TiO_2@ZnIn_2S_4$	300 W Xe lamp $\lambda \geq 420$ nm	618	[12]
$LaVO_4$/g-C_3N_4	300 W Xe lamp	950	[13]
g-C_3N_4/rGO/PDIP	300 W Xe lamp $\lambda \geq 420$ nm	632	[14]
CdS/TiO_2	300 W Xe lamp $\lambda \geq 420$ nm	1780	[15]
$Bi_2Fe_4O_9@ZnIn_2S_4$	**300W Xenon lamp $\lambda \geq 420$ nm**	**3964.26**	**This work**

References

[1] L. Chen, B. Xu, M. M. Jin, L. J. Chen, G. Y. Yi, B. L. Xing, Y. L. Zhang, Y. F. Wu and Z. H. Li, *J. Mol. Struct.,* 2023, **1278**, 134911.

[2] Y. M. Cao, L. Yue, Z. X. Li, Y. H. Han, J. Lian, H. P. Qin and S. Y. He, *Appl. Surf. Sci.,* 2023, **609**, 155191.

[3] Z. Y. Li, H. F. Ma, L. H. Zang, S. Z. Guo and L. L. Shi, *Sep. Purif. Technol.,* 2021, **276**, 119355.

[4] M. Liaqat, N. R. Khalid, M. B. Tahir, S. Znaidia, H. Alrobei and M. Alzaid, *Ceram. Int.,* 2023, **49**, 10455-10461.

[5] H. Li, Z. J. Zhu, C. Y. Hu, J. Zheng and B. J. Liu, *Adv. Powder. Technol.,* 2023, 34, 104066.

[6] L. N. Tian, Y. P. Zhang, L. J. Dai, C. H. Xin, Q. Li, Y. T. Tang and X. Yu, *Mater. Lett.,* 2023, **338**, 134055.

[7] S. Naraginti, K. Sathishkumar, F. C. Zhang and X. H. Liu, *Environ. Res.,* 2023, **223**, 115407.

[8] J. Q. Gao, J. B. Xue, Q. Q. Shen, T. W. Liu, X. C. Zhang, X. G. Liu, H. S. Jia, Q. Li and Y. C. Wu, *Chem. Eng. J.*, 2022, **431**, 133281.

[9] G. C. Zuo, Y. T. Wang, W. L. Teo, Q. M. Xian and Y. L. Zhao, *Appl. Catal. B*, 2021, **291**, 120126.

[10] H. Zhao, Z. F. Jiang, K. M. Xiao, H. L. Sun, H. S. Chan, T. H. Tsang, S. J. Yang and P. K. Wong, *Appl. Catal. B*, 2021, **280**, 119456.

[11] H. H. Ou, C. Tang, Y. F. Zhang, A. M. Asiri, M. M. Titirici and X. C. Wang, *J. Catal.*, 2019, **375**, 104-112.

[12] L. Wang, H. Zhou, H. Zhang, Y. Song, H. Zhang and X. Qian, *Inorg. Chem.,* 2020, **59**, 2278.

[13] X. Li, J. D. Hu, T. Y. Yang, X. G. Yang, J. F. Qu and C. M. Li, *Nano Energy*, 2022, **92**, 106714.

[14] X. J. Chen, J. Wang, Y. Q. Chai, Z. J. Zhang and Y. F. Zhu, *Adv. Mater.*, 2021, **33**, 2007479.

[15] X. Luo, Y. M. Ke, L. Yu, Y. Wang, K. P. Homewood, X. X. Chen and Y. Gao, *Appl. Surf. Sci.*, 2020, **515**, 145970.